Bratisl Lek Listy 2010; 111 (1)
4 – 8

PERSPECTIVES

Chromatin texture, DNA index, and S-phase fraction in primary breast carcinoma cells analysed by laserscanning cytometry

Kuliffay P[1], Sanislo L[1], Galbavy S[1,2]

Institute of Laboratory Medicine, St. Elizabeth University College of Health and Social Work, and St. Elizabeth Cancer Institute, Bratislava, Slovakia. **pkulif@ousa.sk**

Abstract: *Objectives:* Laser scanning cytometry (LSC) is a slide-based technique capable of measuring a number of biological parameters both in immobilised cell suspensions and in formalin-fixed paraffin-embedded tissue sections.
Background: High proliferation rate in surgically removed breast tumours is an unfavourable prognostic factor. In node negative cases it can help distinguish patients with higher risk for distant metastases from those with a lower risk.
Patients and methods: In a prospective study we investigated 140 breast tumours, of which 113 were invasive ductal carcinomas, 11 were invasive lobular carcinomas, and 16 tumours were of other histological types. Cells for LSC investigations were prepared from fresh, surgically removed tumours by mechanical disintegration. After fixation the cells were stained with FITC-conjugated anti-cytokeratin (CK-FITC) to distinguish CK+ tumour cells from CK- stroma, and with propidium iodide to stain DNA.
Results: We identified three S-phase fraction (SPF) groups, with low (30 patients), moderate (54 patients), and high SPF (51 patients). Thirty-seven tumours were diploid, 83 were aneuploid, while 5 tumours had a bimodal distribution of DNA content. Chromatin texture values were increasing in the respective subclasses from the hypodiploid group to the tetraploid/hypertetraploid group.
Conclusion: The measurement of DNA content and SPF of tumours by LSC completed by and correlated with other biological properties of the tumour cells may be a useful tool in assessing prognosis and clinical outcome of patients with breast cancer. *(Tab. 5, Fig. 4, Ref. 18).* Full Text (Free, PDF) *www.bmj.sk.*
Key words: breast cancer, laser scanning cytometry, chromatin texture, DNA index, S-phase fraction.

Cancer cells are characterised by a number of biological features that distinguish them from their normal counterparts both on cellular and subcellular levels (1). Malignant transformation is often associated with changes that are commonly referred to as malignancy-associated changes (MACs) (2). The latter may be manifested as changes in cell morphology, partial or whole chromosome sets, or subcellular changes (e.g. chromatin texture, nuclear morphology, nuclear/cytoplasmic ratio, etc.). Until recently they could be studied only by conventional microscopy, which on the one hand definitely provided a wealth of information, but on the other its analysis was rather subjective (3). Advances in digital imaging technologies (such as laser confocal microscopy and laserscanning cytometry) made it possible to study all those subtle changes that now are not only readily visualised as digital images but are also mathematically quantifiable (4, 5).

Laserscanning cytometry (LSC) is a slide-based technique that combines high throughput multiparametric cytometry and morphological cell analysis (6). Among other features, it enables to assess several nuclear properties, such as DNA index, nuclear area, perimeter and nuclear texture (7, 8). Chromatin texture is characterised as the measure of non-uniformity (granularity) of the nuclear matrix as reflected in variations in propidium iodide (PI) staining intensity within a single nucleus. It has been found to carry significant diagnostic information e.g. in bladder carcinoma (9) or cervical cancer (10).

The aim of this study was to investigate the possible relationships between nuclear chromatin texture, ploidy, and S-phase fraction in primary breast cancer cells by means of laserscanning cytometry.

Methods

Patients. One hundred and forty female patients with primary breast carcinoma were enrolled in the study (mean age 60.8 years, range 37–86 years). The patients underwent surgery for tumour between 2005 and 2008 at the St. Elizabeth Cancer Institute, Bratislava. Histopathologically, 113 tumours were invasive

[1]Institute of Laboratory Medicine, St. Elizabeth University College of Health and Social Work and St. Elizabeth Cancer Institute, Bratislava, Slovakia, and [2]Institute of Forensic Medicine, Faculty of Medicine, Comenius University, Bratislava, Slovakia

Address for correspondence: P. Kuliffay, Institute of Laboratory Medicine, St. Elizabeth University College of Health and Social Work and St. Elizabeth Cancer Institute, Heydukova 10, SK-812 50 Bratislava, Slovakia.
Phone: +421.2.59249516

Acknowledgement: This work was supported by Ministry of Health of the Slovak Republic under the project "Correlation of the number of circulating tumour cells in peripheral blood and bone marrow in breast cancer patients".

Tab. 1. Clinico-pathological characteristics of patients (n=140).

Parameter		n	%
Age (years)	≤45	12	8.6
	46–55	35	25.0
	≥56	93	66.4
Histological type of tumour	Invasive ductal carcinoma	113	80.7
	Invasive lobular carcinoma	11	7.9
	Other types	16	11.4
Tumour size (mm)	≤10	7	5.0
	11–20	72	51.4
	≥21	59	42.2
	ND	2	1.4
Metastatic node involvement (number)	0	77	55.0
	1–3	31	22.1
	≥4	21	15.0
	ND	11	7.9
SBR grading	I	15	10.7
	II	76	54.3
	III	32	22.9
	ND	17	12.1

SBR grading – Scarff-Bloom-Richardson, ND – not determined

Tab. 2. Cytometric characteristics of patients (n=140).

Parameter		n	%
DI	Hypodiploid (≤0.95)	15	10.7
	Diploid (0.96–1.04)	37	26.4
	Aneuploid, low (1.05–1.50)	51	36.4
	Aneuploid, high (1.51–1.99)	20	14.3
	Tetraploid/hypertetraploid (≥2.00)	12	8.6
	Multiploid	5	3.6
SPF (%)	Low (≤5.0)	30	21.4
	Moderate (5.1–10)	54	38.6
	High (>10.1)	51	36.4
	ND	5	3.6

DI – DNA index, SPF – S-phase fraction, ND – not determined,

ductal carcinomas, 11 were invasive lobular carcinomas, and 16 tumours belonged to other histological types.

For each patient, biological and clinico-pathological information was recorded, namely age at diagnosis, histological type of tumour, tumour size, histological SBR grade, and axillary lymph node involvement (Tab. 1), as well as a panel of cytometric data such as DNA index, S-phase fraction, nuclear area, and chromatin texture (Tab. 2).

The ethics committee required no written informed consent from the patients because tumour cell analysis was considered part of the diagnostic process.

Specimen preparation. Unfixed tumour fragments were obtained from the operation theatre immediately after resection, placed in physiological saline and processed for laserscanning cytometry analysis on the same day. Tissues were mechanically disintegrated using a razor blade, filtered through six layers of gauze to separate gross cell debris, and the filtrates were allowed to sediment for 15 min at room temperature to obtain monocellular suspension. The supernatants containing single cell suspension were carefully pipetted off and centrifuged at 450 x g for 10 min, then cells were diluted to about 1×10^6 cells/ml and cytocentrifuged at 250 x g for 8 min onto standard microscopic slides. The cells were then fixed in methanol at 4 °C for 30 min.

Diploid human lymphocytes were used as negative control for DNA index, S-phase fraction, nuclear area, and chromatin texture measurements. The lymphocytes were prepared from peripheral blood according to Bergström and Asman (11) with minor modifications, and were run separately under identical instrument settings.

Cell staining. The cells were stained with FITC-conjugated anti-cytokeratin antibody solution (anti-FITC-CK) (clone CK3-6H5, Miltenyi Biotec, Germany) diluted 1:10 in phosphate buffered saline (PBS) at room temperature in the dark for 10 min. Cells were shortly rinsed with PBS and stained with propidium iodide (Sigma-Aldrich, St. Louis, MO.) at the final concentration of 5 μg/ml at room temperature in the dark for 5 min. The slides were then rinsed with PBS, mounted in glycerol and immediately subjected to LSC analysis.

LSC analysis. Cells were analysed cytometrically using a laserscanning cytometer (CompuCyte Inc., Cambridge, MA) equipped with WinCyte PC-based software. Cytoplasmic and nuclear fluorescence were measured. Slides were scanned using a 40 objective and illuminated by an argon laser at 488 nm. Three to four square scan areas of 5 mm^2 each were chosen at random in the cytospin window occupied by cells, and the upper acquisition limit was set to 2×10^3 cells. Each pixel was scanned in a single-pass way. Fluorescence was separated by optical filter transmitting light at 530±30 nm (green fluorescence, FITC) and 625±28 nm (red fluorescence, PI). Contouring of the events was done on a chosen threshold level (1800 in most cases) for the fluorescence of PI-stained nuclei.

After data acquisition, cell populations were gated in a separate window scattergram (green max pixel *vs.* PI integral) to separate cytokeratin-negative (FITC-CK-) cells from cytokeratin-positive (FITC-CK+) cells which were considered to represent the tumour cell population. Two hundred FITC-CK+ cells were selected randomly in each patient cell sample and their respective cytometric values (DNA index, nuclear area, nuclear perimeter, and chromatin texture) were recorded along with histopathological and clinical properties.

Results

DNA index. DNA index was measured in all of the 140 patients. Based on DI values, the whole group was divided into 6 subclasses comprising tumours with DIs ranging from hypodiploid to hypertetraploid cell populations (Tab. 2). The vast majority of tumours gave unimodal histograms with a single G0-G1 peak,

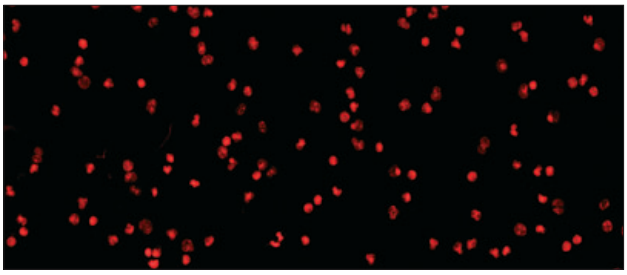

Fig. 1. Diploid lymphocytes. DI=1.00; SPF=0.4; no metastatic involvement. Mean chromatin value 69107.53±29817.85 a. u.

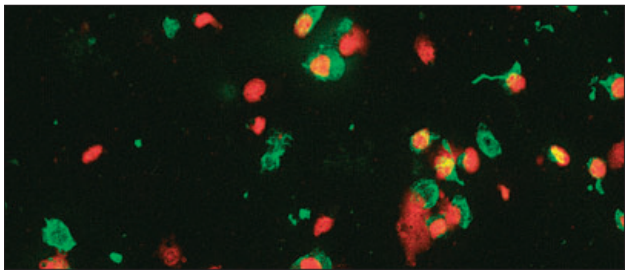

Fig. 3. Invasive ductal carcinoma. DI=1.52; SPF=14.7 %; 4/13 metastases to regional lymph nodes. Mean chromatin value 184045.25±87893.45 a.u.

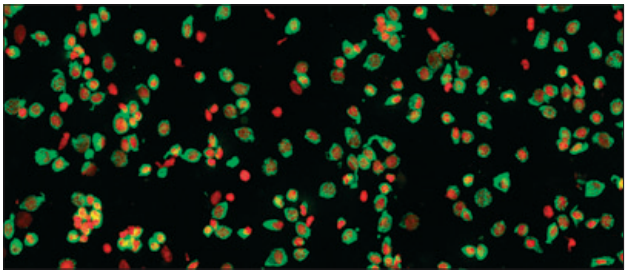

Fig. 2. Invasive ductal carcinoma. DI=1.00; SPF=1.5 %; no metastatic involvement. Mean chromatin value 99641.71±56596.36 a.u.

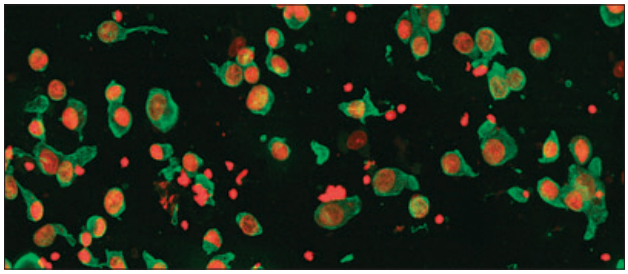

Fig. 4. Invasive ductal carcinoma. DI=2.62; SPF=12.9 %; 10/20 metastases to regional lymph nodes. Mean chromatin value 229950.53±82089.55 a.u.

while there were also 5 multiploid tumours showing more than one (at least two) G0–G1 peaks at various DIs. Two tumour subclasses occurred most frequently: one in the aneuploid region (DI 1.05–1.94, 50.7 %), the other in the diploid/near-diploid region (DI 0.96–1.04, 26.4 %), respectively. The mean CV of the G0–G1 peaks did not exceed 10 %, though its values were lower in the diploid tumours and somewhat higher in the aneuploid subclass.

Chromatin texture. Chromatin texture was expressed numerically in arbitrary units (a.u.) as measured and displayed by the LSC software. The mean values among the respective DNA ploidy subclasses varied greatly, from 105273.84 a.u. in the hypodiploid tumours up to 229950.53 a.u. in the tetraploid subclass (Tab. 3, Figs 1–4). Chromatin texture values in the unimodal groups showed an increasing tendency among the respective subclasses from hypodiploidy to hypertetraploidy.

S-phase fraction. SPF was expressed as percentage of cells being in the S-phase out of all cells being in the cell cycle. As expected, the lowest values were seen in the control cells, while in the tumour cell populations the mean SPF values were increasing with increasing ploidy (Tab. 3). In all tumour subclasses the S-phase fraction had much higher values than the control cells which reflected the proliferation activity of the tumours.

Other cytometric parameters. Also other parameters were investigated cytometrically, such as nuclear area, nuclear perimeter, as well as the texture/area ratio and the nuclear perimeter/area ratio (Tab. 3). Nuclear area and perimeter values were increasing with ploidy, while the texture/area ratios were rather similar among the respective subclasses, and the perimeter/area ratios decreased with ploidy.

Tab. 3. Chromatin texture, SPF, and nuclear area in the respective tumour subclasses based on DI (n=140), and in healthy control subjects (n=15).

DI	n	Chromatin texture (a.u.) (mean±SD)	SPF (%) (mean±SD)	Nuclear area (μm^2) (mean±SD)	Perimeter (μm) (mean±SD)	Texture/Area (mean±SD)	Perimeter/Area (mean±SD)
Hypodiploid (≤0.95)	15	105273.84±42157.55	7.03±2.60	56.84±19.54	109.85±22.21	1889.85±630.44	2.06±0.51
Diploid (0.96–1.04)	37	99641.71±56596.36	7.44±4.79	54.34±20.57	104.10±31.96	1775.88±890.99	1.98±0.34
Aneuploid, low (1.05–1.50)	51	144560.37±73926.54	9.71±6.14	72.86±27.71	120.51±32.01	1882.20±569.27	1.74±0.32
Aneuploid, high (1.51–1.99)	20	184045.25±87893.45	12.03±8.61	89.04±29.47	133.57±33.58	2008.43±651.34	1.57±0.33
Tetraploid/hypertetraploid (≥2.00)	12	229950.53±82089.55	11.89±5.92	115.47±31.98	143.18±26.01	1900.53±362.82	1.29±0.24
Multiploid (various Dis)	5	172292.46±102716.91	11.64±7.52	86.83±39.50	121.07±28.76	1826.94±509.91	1.53±0.36
Diploid control	15	69107.53±29817.85	1.2±0.7	38.33±7.37	77.80±8.66	1697.40±578.22	2.07±0.24

SPF – S-phase fraction, DI – DNA index

Tab. 4. DNA index and metastatic lymph node involvement in breast cancer patients (n=137).

DI	n[1]	%
Hypodiploid (≤0.95)	5/15	33.3
Diploid (0.96-1.04)	14/37	37.8
Aneuploid, low (1.05–1.50)	7/44	38.6
Aneuploid, high (1.51–1.99)	11/29	37.9
Tetraploid/hypertetraploid (≥2.00)	7/12	58.3

DI – DNA index, [1]ratio of lymph node positive patients to all patients in the subclass

Tab. 5. S-phase fraction and metastatic lymph node involvement in breast cancer patients (n=137).

SPF (%)		n[1]	%
< 5	low	9/30	30.0
5.1-10	moderate	20/55	36.4
>10.1	high	21/52	40.4

SPF – S-phase fraction, 1ratio of lymph node positive patients to all patients in the subclass

Axilllary lymph node status. Axillary lymph node involvement was slightly increasing with DNA ploidy (Tab. 4), the lowest involvement being in the hypodiploid subclass (33.3%), while the highest value was found in the tetraploid/hypertetraploid subclass (58.3 %). Likewise, lymph node involvement was increasing with increasing SPF values from 30.0 % in the low SPF group to 40.4 % in the high SPF group (Tab. 5).

Discussion

Laser-scanning cytometry is a rather novel tool in the field of cytometric investigations. In contrast to flow cytometry, LSC is slide-based which enables to examine cell populations not in suspension but on a standard microscopic slide (12). Beside all those common features that are offered by flow cytometry (e.g., apoptosis, immunophenotyping, circulating tumour cells, DI, SPF, etc.), LSC provides a unique property, namely the possibility to relocalise and measure every cell repeatedly in new staining settings; moreover it enables to measure reliably as many as several hundred events. However, despite all these unique features of LSC it might be employed more advantageously in routine cytological investigations rather than in routine pathology (13).

Currently, the most frequently used feature of LSC is the determination of DNA index and S-phase fraction in tumour cell populations, either freshly prepared from bioptical material, or prepared from formalin-fixed, paraffin-embedded archival material (14). DNA index and SPF are generally accepted prognosticators in many tumour localisations (15–18), Welkoborsky et al, 1999; Millot a Dufer, 2000).

In our prospective study, we investigated 140 female patients with breast carcinoma. Beside DNA index and SPF, we also analysed other features offered by LSC, such as chromatin texture, nuclear area, nuclear perimeter, or their various ratios calculated per nuclear area, respectively.

Chromatin texture is one of those cellular properties that are believed to be malignancy-related and are often referred to as malignancy-associated changes (MACs) (Sun et al, 2003) that may be microscopically manifested as changes in cell morphology, partial or whole chromosome sets, or even changes on the subcellular level. Until recently, these changes could be studied only by conventional light microscopy, which definitely provides a wealth of information, yet the analysis of these alterations is potentially subject to considerable bias (Basiji et al, 2007). Although it is almost generally accepted that elevated chromatin texture values as MAC are associated with poorer prognosis, to our knowledge, only very few literature data are available on this topic. In our group of breast cancer patients we found that chromatin texture values increased with tumour ploidy and was a function of nuclear size, rather than a function of MACs reflected also in corresponding metastatic lymph node involvement.

It has been demonstrated that cancer patients with aneuploid tumours or tumours with higher ploidy levels tend to have a poorer prognosis. In our group of patients, it was not yet possible to analyse the survival because the first patients were included in the cohort only in 2005. However, the assessment of axillary lymph node involvement in the respective DI subclasses showed that the lowest metastatic involvement was in the hypodiploid group (33.3 %) and the highest in the tetraploid/hypertetraploid group (58.3 %) (Tab. 4); nevertheless these patients had been neither subdivided further according to histological type of tumour, nor age-matched. A similar relationship was seen when SPF and lymph node involvement were correlated: in the subclass with low SPF, 30.0 % of the patients had positive lymph node status, while in the high SPF subclass this proportion was 40.4 %.

References

1. Hoque A, Lippman SM, Boiko IV et al. Quantitative nuclear morphometry by image analysis for prediction of recurrence of ductal carcinoma in situ of the breast. Cancer Epidemiol Biomarkers Prev 2001; 10: 249—259.

2. Sun XR, Zheng Y, MacAuley C, Lam S, Doudkine A, Palcic B. In vitro model for studying malignancy associated changes. Anal Cell Pathol 2003; 25: 95—102.

3. Basiji DA, Ortyn WE, Liang L, Venkatachalam V, Morrissey, P. Cellular image analysis and imaging by flow cytometry. Clin Lab Med 2007; 27: 653—670.

4. Gil J, Wu, HS. Applications of image analysis to anatomic pathology: Realities and promises. Cancer Invest 2003; 21: 950—959.

5. Carpenter AE, Jones TR, Lamprecht MR et al. CellProfiler: image analysis software for identifying and quantifying cell phenotypes. Genome Biol 2006; 7: R100.

6. Mosch B, Mittag A, Lenz D, Arendt T, Tárnok A. Laser scanning cytometry in human brain slices. Cytometry Part A 2006; 69A: 135—138.

7. Arocena DG, Iwahashi CK, Won N et al. Induction of inclusion formation and disruption of lamin A/C structure by premutation CGG-repeat RNA in human cultured neural cells. Hum Mol Genet, 14: 2005, 3661—3671.

8. Galbavy S, Kuliffay P. Laser scanning cytometry (LSC) in pathology – a perspective tool for the future? Bratisl Lek Listy 2008; 109: 3—7.

9. van Velthoven R, Petein M, Zlotta A et al. Computer-assisted chromatin texture characterization of Feulgen-stained nuclei in a series of 331 transitional bladder carcinomas. J Pathol 1994; 173: 235—242.

10. Walker RF, Jackway PT, Lovell B. Cervical cell classification via co-occurrence and markov random field features. In: Proceedings of DICTA-95, Digital Image Computing: Techniques and Applications, 294—299, Brisbane, Australia, 30 Nov—2 Dec 1995.

11. Bergstrom K, Asman B. Luminol enhanced Fc-receptor dependent chemiluminescence from peripheral PMN cells. A methodological study. Scand J Clin Lab Invest 1993; 53: 171—177.

12. Gerstner AOH, Muller AK, Machlitt J, et al. Slide-based cytometry for predicting malignancy in solid salivary gland tumors by fine needle aspirate biopsies. Cytometry Part B 2003; 53B: 20—25.

13. Gerstner AOH, Tarnok A. Analysis of fine-needle aspirate biopsies from solid tumors by laser scanning cytometry (LSC). Current Protocols in Cytometry 2002; 7.20.1—7.20.10.

14. Kamada T, Sasaki K, Tsuji T, Todoroki T, Takahashi M, Kurose A. Sample preparation from paraffin-embedded tissue specimens for laser scanning cytometric DNA analysis. Cytometry 1997; 27: 290—294.

15. Franzen G, Klausen OG, Grenko RT, Carstensen J, Nordenskjold B. Adenoid cystic carcinoma: DNA as a prognostic indicator. Laryngoscope 1991; 101: 669—673.

16. Hemmer J, Thein A, van Heerden WFP. The value of DNA flow cytometry in predicting development of lymph node metastasis and survival in patients with locally recurrent oral squamous cell carcinoma. Cancer 1997; 79: 2309—2313.

17. Welkoborsky HJ, Gluckmann JL, Jacob R, Bernauer H, Mann W. Tumor biologic prognostic parameters in T1N0M0 squamous cell carcinoma of the oral cavity. Laryngorhinootologie 1999; 78: 131—138.

18. Millot C, Dufer J. Clinical applications of image cytometry to human tumour analysis. Histol Histopathol 2000; 15: 1185—1200.

Received September 20, 2009.
Accepted November 2, 2009.